Title
Circular Dichroism in Off-Resonantly Coupled Plasmonic Nanosystems.

Journal
Nano letters, 15(12)

ISSN
1530-6984

Authors
Ferry, Vivian E
Hentschel, Mario
Alivisatos, A Paul

Publication Date
2015-12-01

DOI
10.1021/acs.nanolett.5b03970

Peer reviewed

NANO LETTERS

Letter

pubs.acs.org/NanoLett

Circular Dichroism in Off-Resonantly Coupled Plasmonic Nanosystems

Vivian E. Ferry,[†,#] Mario Hentschel,[‡,#] and A. Paul Alivisatos*[,‡,§,∥,⊥]

[†]Department of Chemical Engineering and Materials Science, University of Minnesota—Twin Cities, 421 Washington Ave SE, Minneapolis, Minnesota 55455, United States

[‡]Materials Science Division, Lawrence Berkeley National Laboratory, 1 Cyclotron Road, Berkeley, California 94720, United States

[§]Department of Chemistry, University of California, Berkeley, California 94720, United States

[∥]Department of Materials Science, University of California, Berkeley, California 94720, United States States

[⊥]Kavli Energy NanoScience Institute, University of California, Berkeley, California 94720, United States

S *Supporting Information*

ABSTRACT: Chiral plasmonic systems have been shown to exhibit large chiroptical responses, much larger than those found in molecular or solid state systems. In this Letter, we investigate the role of resonant coupling in such systems and whether the formation of collective plasmonic modes in a chiral assembly of metallic nanostructures is a necessary condition for chiroptical response. We show in experiment and simulation that off-resonant coupling between spectrally detuned nanostructures arranged with structural chirality leads to a clear but weak chiroptical response. We interpret our results in the framework of scattering between the individual constituents that in turn leads to a chiroptical farfield response. We envision that our results will allow further tuning and manipulation of chiroptical responses in plasmonic systems for tailored chiral light matter interaction.

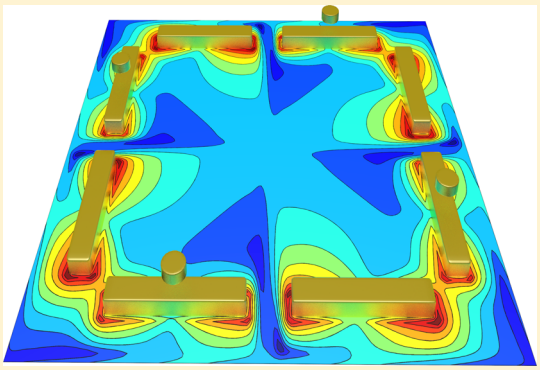

KEYWORDS: *surface plasmons, circular dichroism, chirality, plasmon hybridization*

Chiral objects, which cannot be superimposed on their mirror image, are important across a range of length scales, from atomic scale examples of amino acids and asymmetric catalysts to macroscopic examples such as propellers. One of the key benefits of chiral media for photonics is polarization selectivity: the enantiomers interact distinctly with right and left handed circularly polarized light. The optical response of chiral materials has recently been studied in detail in nanoscale plasmonic systems, where key studies have shown significantly enhanced chiroptical response as compared to molecular systems. Although molecular systems typically exhibit anisotropy factors of 10^{-2}–10^{-3}, anisotropy factors of 2% or higher are realizable in plasmonic systems.[1,2] One reason for this difference is related to the large polarizability of the plasmonic resonance that fundamentally stems from the large number of quasi-free conduction electrons. A second factor is the longer length scale of plasmonic chiral systems compared to molecular systems, which is closer to the length scale of the helical pitch of circularly polarized light.[3,4]

In molecular systems, chiroptical response may arise from many different interactions. For example, achiral chromophores positioned in a chiral arrangement can couple together, inducing a chiroptical response for the system. These chromophores could have degenerate energies, as in biphenyl, or nondegenerate energies, with the nondegenerate case showing weaker chiroptical response. An example of this type of interaction is induced chirality in host−guest systems such as cyclodextrin: here the chiral host imparts chirality onto the guest molecule, which is observed through chiroptical response at the energy of the guest.[5,6]

Similarly to the chromophores in molecular systems, achiral plasmonic nanostructures arranged in chiral unit cells can couple together to produce a chiroptical response. In this type of assembly, the chiroptical response typically results from the formation of hybridized plasmonic modes between resonantly matched nanostructures, with the strongest response occurring when the nanostructures are close together.[7] In this paper, we instead investigate the plasmonic analog to the nondegenerate chromophore case and study the chiroptical response when the resonances of the constituents are intentionally detuned.[8] In this case, the plasmonic nanostructures interact via the light field rather than through hybridization. In contrast to the plasmonic systems formed by hybridization, this is a weak interaction.

Received: September 30, 2015
Revised: November 11, 2015
Published: November 16, 2015

DOI: 10.1021/acs.nanolett.5b03970
Nano Lett. 2015, 15, 8336−8341

The key difference between solid state or molecular systems and their plasmonic analogs is the ease of tuning resonance energies; simply by changing the size of a plasmonic nanostructure, for example, the resonance position can be significantly shifted. By the same token, if differently sized plasmonic nanostructures are used in assemblies, there is no guarantee that the elements will interact or form collective plasmonic modes. Although weak, this may have important consequences for the design of chiroptical plasmonic assemblies.

Figure 1 shows a schematic overview contrasting different chiral plasmonic systems. The simplest example of a chiral

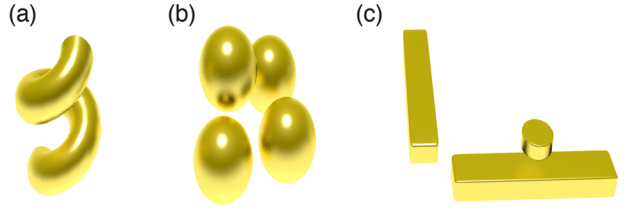

Figure 1. Sketches of different chiral plasmonic structures. (a) Object with individual chirality, such as a spiral. (b) Chiral system formed from the arrangement of four identical nanoparticles on the edges of an asymmetric tetramer. The nanoparticles form hybridized plasmonic modes that give rise to a chiroptical response. (c) Chiral system consisting of spectrally detuned plasmonic structures, which interact via the light field rather than the formation of hybridized modes.

plasmonic system is an individually chiral nanostructure, such as a spiral,[9−11] gammadion-like system,[12−15] or similar (Figure 1a).[16] The second image (Figure 1b) denotes a chiral assembly where the resonances of all the constituents are matched, such as the structure where four identical nanoparticles are arranged on a distorted tetrahedral frame.[2,17−25] Figure 1c depicts our geometry. A single gold nanodisk is positioned above an L-shape consisting of two individual gold nanorods. Depending on the position of the gold nanodisk in the upper layer, the overall geometry can be left- or right handed as well as achiral. The plasmonic resonance of the nanodisk is significantly spectrally detuned from the plasmonic modes of the nanorods (see also Supporting Information). Figure 2a shows the experimental scanning electron micrograph of the fabricated structures, which are fabricated with 4-fold rotation to avoid measurement errors.[26] Figure 2b shows the measured far-field optical response under left- and right-hand polarized (LCP, RCP) excitation of the system. Two modes are observed around 2000 nm, which correspond to the symmetric and antisymmetric combination of the dipolar plasmon modes of the nanorods. When the LCP and RCP spectra are examined closely, small differences indicating a chiroptical response are evident.

The chiroptical response, defined as the difference in transmittance for RCP and LCP incoming light, is shown in Figure 3a. We fabricated the two enantiomers of the assembly as well as an achiral arrangement with the dot located in the center of the two bars, as shown in the scanning electron microscope image in Figure 3c. The chiroptical response is primarily observed at the same spectral positions as the modes in Figure 2. As expected, the chiroptical response exhibits opposite sign for the two enantiomers and vanishes for the achiral geometry.

To probe the mechanism producing this chiroptical response, we first changed the size of the upper layer nanodisk and

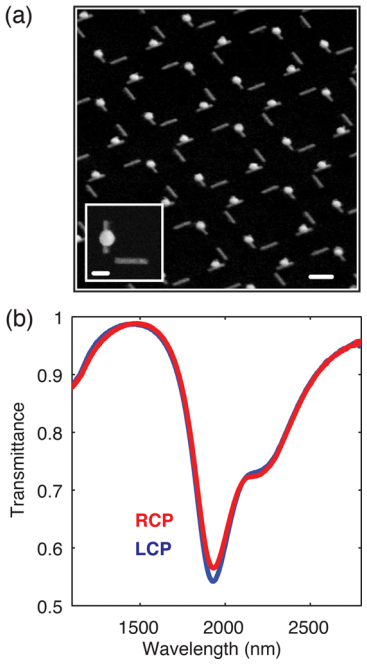

Figure 2. (a) Investigated structures that consist of a bottom layer of two individual Au nanorods forming an L-shape, and a single Au nanodisk positioned above the L-shape in an upper layer. The position of the nanodisk renders the structure chiral or achiral. Overview and close-up SEM micrographs of the investigated nanostructures. The individual nanorods have a length of 370 nm, width of 70 nm, and thickness of 40 nm. The gap width is 70 nm. The nanodisk has a diameter of 180 nm and thickness of 60 nm. Vertical spacing distance is 70 nm. Periodicity is 1000 nm. Scale bars are 200 nm in the inset and 500 nm for the overview image. (b) Experimental transmittance spectra for RCP and LCP light. Two modes can be observed around 2000 nm that correspond to the symmetric and antisymmetric combination of the fundamental dipolar plasmon modes.

compared the spectra. The nanorod dimensions are identical in both cases, and nanodisk diameters of 180 and 100 nm were fabricated. Examining the spectra in Figure 3a and d, we observe that the amplitude of the chiroptical response has decreased, but there is no shift in the spectral positions. If the three nanostructures formed a collective plasmonic mode, we should observe spectral shifts and changes in the mode structure of the system due to the shifted resonance of the nanodisk. If instead there is no resonant interaction and, therefore, no formation of a collective plasmonic mode shared between all three nanostructures, the mode structure of the chiroptical response should not change as the resonance of the top disk shifts. In this case, decreasing the size of the upper layer nanodisk should decrease the amplitude of the chiroptical response, as observed. Under this mechanism, the upper nanodisk interacts with the nanorods in two ways: first, the incident radiation is scattered by the disk before interacting with the nanorod, and second, radiated light from the nanorod may be rescattered by the nanodisk. Decreasing the size of the nanodisk decreases its off-resonant scattering cross section, which should influence both interactions.

We also performed numerical simulations of the chiroptical response using the finite difference time domain method to calculate the transmission spectra under LCP and RCP excitation. The calculated chiroptical response is shown in Figure 3b and e for structures with the corresponding dimensions to the experiment and agrees well with the

DOI: 10.1021/acs.nanolett.5b03970
Nano Lett. 2015, 15, 8336−8341

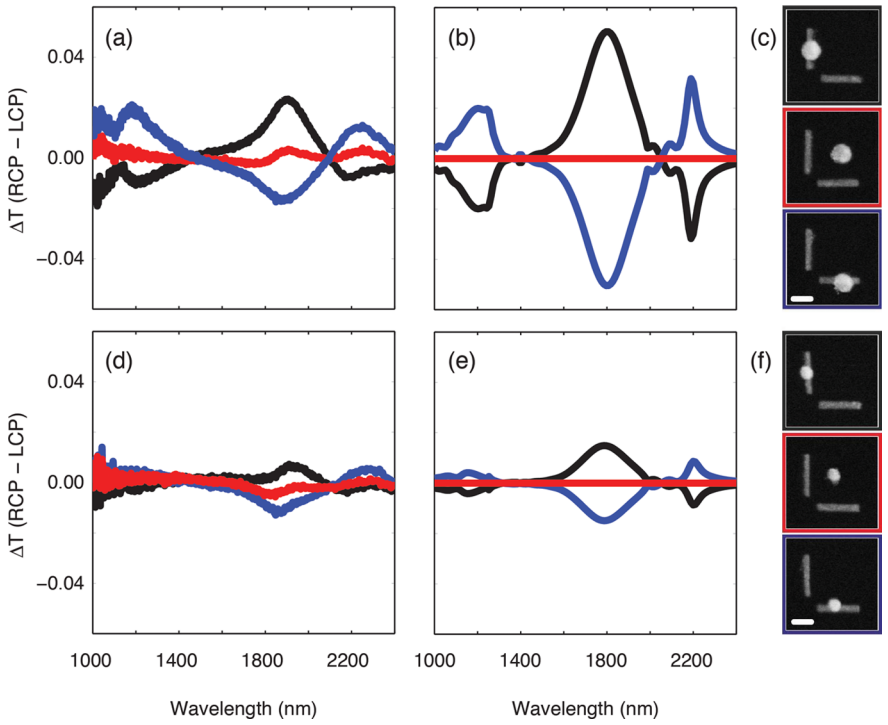

Figure 3. Experimental and simulated chiroptical response, defined as the difference of the transmittance for RCP and LCP excitation. The colored frames around the SEM images correspond to the colors of the shown spectra and apply to the simulations as well as the experiment. Panels a and b depict the spectra for an upper layer nanodot of 180 nm size, panels d and e for a diameter of 100 nm. Panels c and f show SEM images of the corresponding structures. We observe a clear chiroptical response that changes sign for interchanged structural handedness and vanishes in case of the achiral structure. Reducing the size of the upper layer nanodot does not change the modes structure of the spectra but reduces the overall amplitude of the chiroptical response. This behavior is consistent with an off-resonant interaction between the bottom layer nanorods and the upper layer nanodisk.

experimental measurements. The overall mode structure and the spectral position as well as the relative amplitudes are well reproduced. Importantly, both features of the proposed off-resonant interaction are clearly visible: the spectral features do not shift when reducing the dimension of the upper layer nanodisk, and the amplitude of the chiroptical response decreases with decreasing nanodisk diameter.

Using simulation, we calculated the chiroptical response as a function of the diameter of the upper layer nanodisk across a broader range of sizes. The resulting spectra are shown in Figure 4 as a 2D color plot, where it is evident that the mode structure of the chiroptical response is not changed across a wide range of nanodisk sizes despite the significant shift in nanodisk resonance wavelength. If there were a remaining resonant interaction between all three nanostructures, then variation of the nanodisk diameter between 60 and 180 nm would reveal a change in the spectral features. Figure 4 also shows a significant increase in the amplitude of the chiroptical response with increasing diameter. As discussed above, this behavior is in accordance with our expectation as the increased geometrical size corresponds to an increased scattering cross section, which interacts with a larger portion of the incoming and rescattered intensity. The larger nanodisks, therefore, increase the chiroptical response of the system. We have also performed simulations of the individual subsystems, that is, the pair of nanowires in the first layer and the single nanodisk in the second layer. The simulated extinction cross section sectra are shown in the Supporting Information Figure S1. Even for the largest nanodisk diameter of 180 nm studied in the

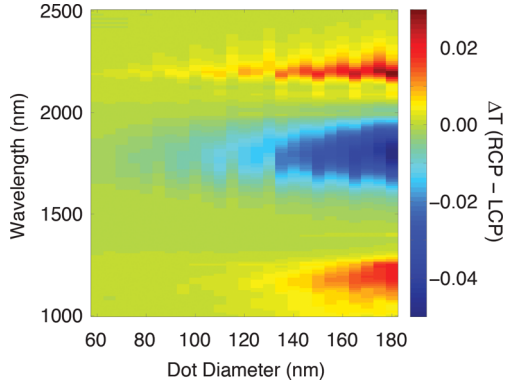

Figure 4. Simulated chiroptical response for different diameters of the upper layer nanodisk. Each slice along the *y* axis corresponds to a spectrum for a given nanodisk diameter. As can be seen, the shape of the spectra do not change over this range of sizes, proving that there is no hybrid mode formation between the L-shape and the nanodisk. However, we observe an increase in the overall amplitude of the response that stems from the increased size and thus off-resonant interaction with the nanodisk.

manuscript, the resonances are spectrally well separated and no resonance overlap is observed.

To examine the response of the assemblies in more detail, we calculated the near field distributions from simulation. Figure 5 shows the magnitude of the electric field in the assemblies, comparing the near-field response of the assemblies with and without the upper layer nanodisk. The nanodisk is 180 nm in diameter, as in the preceding experimental example. The field

DOI: 10.1021/acs.nanolett.5b03970
Nano Lett. 2015, 15, 8336−8341

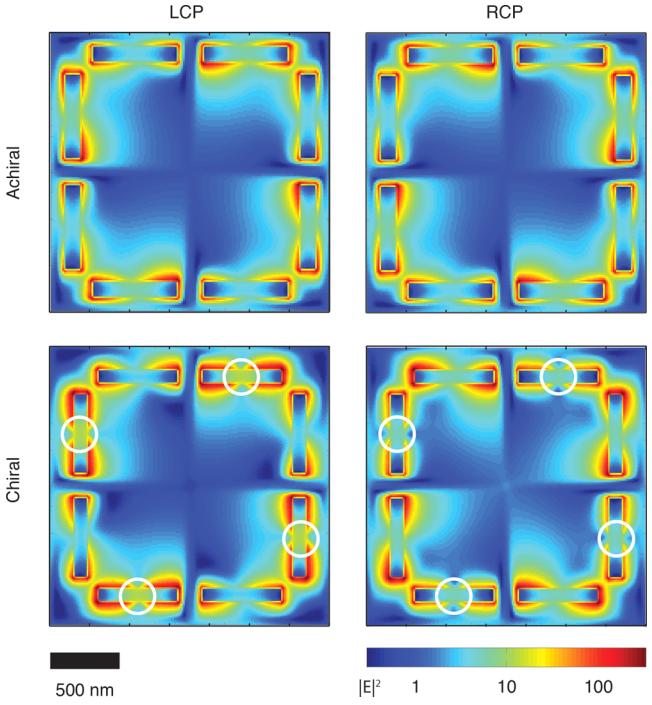

Figure 5. Simulated electric field distributions (magnitude of **E**, at 1797 nm, the calculated maximum chiroptical response) for the L-shape layer alone (upper row) and for the chiral arrangement with a 180 nm nanodisk present in the second layer (white outline). The images are $x-y$ cross sections taken at the height of the top of the bar in the lower layer. In the chiral case, the position of the upper level nonresonant nanodisks is shown with a white outline. It is apparent that the presence of the upper layer nanodot does not significantly influence the nature of the plasmonic modes. As the overall nature of the modes remains unchanged, this indicates that the upper layer nanodisk does not form a resonantly coupled mode with the underlying nanorods.

profiles shown are $x-y$ maps taken at the z position equal to the top of the nanobars, at the wavelength of the maximum chiroptical response (1797 nm). A full unit cell of the geometry, corresponding to four assemblies with 4-fold rotation, is shown. The upper row depicts the near field distributions under LCP and RCP excitation for an achiral assembly consisting of only the lower layer nanorods. The individual bars show dipolar plasmon excitations, as expected. In the lower row, near field distributions for the chiral assembly containing an upper layer nanodisk are shown; the position of the nanodisk in the upper layer is depicted with a white circle. The nanodisk is positioned in the minimum of the electric field distribution of the dipolar excitations and, consequently, only marginally changes the overall electric field distribution. Importantly, the field distribution continues to resemble two coupled dipolar resonances rather than the distribution expected for collective mode formation between all three nanostructures. However, small changes and differences in the field distributions are evident. In particular, the overall asymmetry of the modes under RCP and LCP excitation increases, showing that the field distribution becomes of chiral character in the presence of the upper layer nanodisk. This is consistent with off-resonant scattering by the gold nanodisk. A portion of the incoming field and of the radiated fields are shielded and rescattered by the nanodisk, thus rendering the scattered intensity distribution chiral. This behavior manifests itself also in the near-fields of the individual dipolar nanorods and explains the observed chiral response despite the lack of collective mode formation.

From a purely geometrical point of view, the structural handedness of the arrangement becomes largest when the nanodisk is positioned over end tip of the nanorods, but we find that the maximum chiroptical response occurs when the nanodisk is positioned over the center of the nanorods. Figure 6a shows the results of a simulation where we shifted the

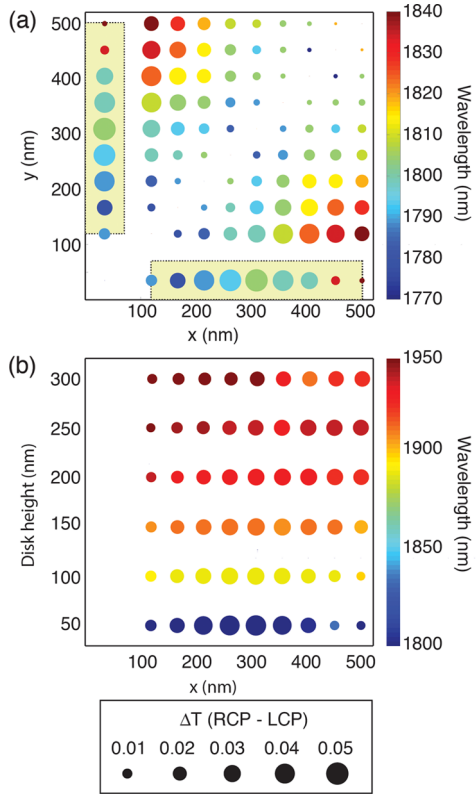

Figure 6. Simulated chiroptical response in dependence of the position of the upper layer nanodisk. (a) Maximum chiroptical response (ΔT) and its spectral position for a position variation in the horizontal $x-y$ plane (the gray outline indicate the position of the nanobars). (b) Maximum of the chiroptical response for different z heights over the x-oriented nanobar.

position of the upper layer nanodisk in two dimensions in the plane above the L-shape. As we cannot plot the full spectral information for each nanodisk location, we instead show the magnitude and spectral position of the main peak in the chiroptical response (located at 1797 nm in Figure 3). The magnitude of the chiroptical response is encoded in the size of the dot, the spectral position is encoded in the color, and the spatial position corresponds to the spatial position of the disk in the plane above the L-shape. Each marker is thus the result of two simulations (RCP and LCP excitation) on a single structure.

First, we see that the chiroptical response vanishes for all positions along the diagonal between the two dipolar nanorods, as expected for these achiral arrangements. Examining the chiroptical response as the upper layer nanodisk is shifted along the length of one nanorod, we see that the chiroptical response reaches a maximum when the nanodisk is in the middle of the nanorod and decreases again toward the end of the rod. Also,

DOI: 10.1021/acs.nanolett.5b03970
Nano Lett. 2015, 15, 8336−8341

we observe a significant red spectral shift of the maximum chiroptical response as the nanodisk shifts toward the end of the nanorod. Although the decreased chiroptical response toward the end of the nanorod is unexpected from a geometrical standpoint, this finding is consistent with the off-resonant interaction argument. When the disk is located above the end of the nanorod, it is located in a region of high field strength (Figure 5). Though this position would be desirable in cases of resonant mode formation as it maximizes the interaction, it is counterproductive in the present situation because it acts as a high effective refractive index material that detunes one nanorod relative to the other nanorod. The presence of a perturbing refractive index also explains the spectral red shift. Therefore, in this case, the middle position of the disk is favorable for the chiroptical response, as it balances the requirement of symmetry breaking with the one for the least refractive index interaction.

Using this argument, we would then expect that increasing the distance between the upper layer nanodisk and the nanorods should shift the location of maximum chiroptical response toward the edge of the nanorod, the point of maximum structural chirality. We performed this calculation for a shift in nanodisk position above one nanorod for different vertical distances, shown in Figure 6b, where the size of the marker corresponds to the magnitude of the chiroptical response at the maximum, and the color again corresponds to the wavelength of the maximum chiroptical response. Each point is again the result of two simulations performed on the full unit cell. As the vertical distance between the nanorod and nanodisk increases, we observe a shift of the maximum chiroptical response toward the end of the nanorod, along with an overall decrease in the maximum response. This result is consistent with our previous explanation, as the near field of the nanorods decays strongly with distance. At the largest distances, it is no longer necessary for the nanodisk to be located in the minimum of the field strength, as there is little field strength present at any length along the nanorod, and the maximum chiroptical response is observed at the same position as the maximum structural chirality. However, the amplitude of the chiroptical response will also decrease as the nanodisk can rescatter less of the radiation from the nanorods. The overall chiroptical effect is reduced.

In conclusion, we have demonstrated in experiment and simulation a chiral optical response in an off-resonantly coupled system comprising of two resonantly coupled nanorods and a single nanodisk. The two nanorods are achiral entities and the overall arrangement is rendered chiral solely by the presence of the off-resonant nanodisk. We have shown that the phenomenon is caused by the off-resonant scattering of the incoming light and rescattering of light off of the nanodisk rather than by the formation of a collective chiral mode. It is important to note, however, that the chiroptical response is weak compared to resonantly coupled plasmonic systems and/or systems exhibiting collective modes with a chiral nature. We therefore expect that the response of a fully off-resonant system, that is, a system in which we also detune the two nanorods from each other, will even be weaker. We also note that it is not necessary that all of the nanostructures in the assembly consist of the same material, or even that they all consist of plasmonic metals. This fundamental finding may aid in the design of chiral plasmonic systems for a tailored light−matter interaction.

Methods. *Simulations.* All simulations were performed using Lumerical FDTD software. The complex refractive index of the Au nanostructures was modeled using a Lorentz−Drude fit to the complex refractive index data given in Palik.[27,28] Two simulations were run on each structure with different circular polarization of the incident light, and the difference in the resulting transmission spectra are shown as the chiroptical response. One unit cell in the simulation corresponds to four assemblies, arranged with C4 rotation as in the experiment.

Fabrication. First, a glass substrate is coated with a 120 nm thick dielectric layer by spin-coating (IC1-200, Futurrex). The gold structures are defined by electron beam lithography (Crestec CABL-9510CC) in a positive resist (PMMA, Microchem) followed by thermal evaporation of a 3 nm of Ti adhesion layer and 40 nm of gold followed by a lift-off procedure. Subsequently, the sample is coated with another 60 nm thick dielectric layer. In order to promote adhesion of the dielectric layer we utilized an adhesion promoter (SurPass 3000, DisChem). The second layer is exposed in an aligned second electron beam lithography step, followed by evaporation (3 nm of Ti and 60 nm of Au), lift-off, and a final planarization step. The footprint of each array is $30 \times 30\ \mu m^2$.

Measurement. The optical response was evaluated using a Fourier-transform infrared spectrometer, combined with an infrared microscope giving extinction (1-transmittance) spectra. The polarization was set with an infrared polarizer and a broadband quarter waveplate (Thorlabs).

■ ASSOCIATED CONTENT

Supporting Information

The Supporting Information is available free of charge on the ACS Publications website at DOI: 10.1021/acs.nanolett.5b03970.

Simulated extinction cross section spectra of the single upper layer nanodisk and the first layer pair of nanobars. (PDF)

■ AUTHOR INFORMATION

Corresponding Author

*E-mail: alivis@berkeley.edu.

Author Contributions

#(V.E.F. and M.H.) These authors contributed equally.

Notes

The authors declare no competing financial interest.

■ ACKNOWLEDGMENTS

M.H. gratefully acknowledges financial support by the Alexander von Humboldt Foundation through a Feodor Lynen scholarship. This material is based upon work supported by the National Science Foundation under Grant DMR-1344290. The authors acknowledge the Marvell Nanofabrication Laboratory for the use of their facilities and the group of Xiang Zhang for the use of their FTIR spectrometer.

■ REFERENCES

(1) McPeak, K. M.; van Engers, C. D.; Blome, M.; Park, J. H.; Burger, S.; Gosálvez, M. A.; Faridi, A.; Ries, Y. R.; Sahu, A.; Norris, D. J. *Nano Lett.* **2014**, *14*, 2934−2940.

(2) Kuzyk, A.; Schreiber, R.; Fan, Z.; Pardatscher, G.; Roller, E.-M.; Högele, A.; Simmel, F. C.; Govorov, A. O.; Liedl, T. *Nature* **2012**, *483*, 311−314.

(3) Tang, Y.; Cohen, A. E. *Science* **2011**, *332*, 333−336.

(4) Valev, V. K.; Baumberg, J. J.; Sibilia, C.; Verbiest, T. *Adv. Mater.* **2013**, *25*, 2517−2534.

DOI: 10.1021/acs.nanolett.5b03970
Nano Lett. 2015, 15, 8336−8341

(5) Liu, M.; Zhang, L.; Wang, T. *Chem. Rev.* **2015**, *115*, 7304−7397.
(6) Allenmark, S. *Chirality* **2003**, *15*, 409−422.
(7) Hentschel, M.; Schäferling, M.; Weiss, T.; Liu, N.; Giessen, H. *Nano Lett.* **2012**, *12*, 2542−2547.
(8) Duan, X.; Yue, S.; Liu, N. *Nanoscale* **2015**, *7*, 17237.
(9) Gansel, J. K.; Thiel, M.; Rill, M. S.; Decker, M.; Bade, K.; Saile, V.; von Freymann, G.; Linden, S.; Wegener, M. *Science* **2009**, *325*, 1513−1515.
(10) Kaschke, J.; Blome, M.; Burger, S.; Wegener, M. *Opt. Express* **2014**, *22*, 19936.
(11) Radke, A.; Gissibl, T.; Klotzbücher, T.; Braun, P. V.; Giessen, H. *Adv. Mater.* **2011**, *23*, 3018−3021.
(12) Kuwata-Gonokami, M.; Saito, N.; Ino, Y.; Kauranen, M.; Jefimovs, K.; Vallius, T.; Turunen, J.; Svirko, Y. *Phys. Rev. Lett.* **2005**, *95*, 227401.
(13) Decker, M.; Klein, M. W.; Wegener, M.; Linden, S. *Opt. Lett.* **2007**, *32*, 856.
(14) Hendry, E.; Carpy, T.; Johnston, J.; Popland, M.; Mikhaylovskiy, R. V.; Lapthorn, A. J.; Kelly, S. M.; Barron, L. D.; Gadegaard, N.; Kadodwala, M. *Nat. Nanotechnol.* **2010**, *5*, 783−787.
(15) Schwanecke, A. S.; Krasavin, A.; Bagnall, D. M.; Potts, A.; Zayats, A. V.; Zheludev, N. I. *Phys. Rev. Lett.* **2003**, *91*, 247404.
(16) Fan, Z.; Govorov, A. O. *Nano Lett.* **2012**, *12*, 3283−3289.
(17) Shen, X.; Song, C.; Wang, J.; Shi, D.; Wang, Z.; Liu, N.; Ding, B. *J. Am. Chem. Soc.* **2012**, *134*, 146−149.
(18) Fan, Z.; Govorov, A. O. *J. Phys. Chem. C* **2011**, *115*, 13254−13261.
(19) Guerrero-Martínez, A.; Auguié, B.; Alonso-Gómez, J. L.; Džolić, Z.; Gómez-Graña, S.; Žinić, M.; Cid, M. M.; Liz-Marzán, L. M. *Angew. Chem., Int. Ed.* **2011**, *50*, 5499−5503.
(20) Shemer, G.; Krichevski, O.; Markovich, G.; Molotsky, T.; Lubitz, I.; Kotlyar, A. B. *J. Am. Chem. Soc.* **2006**, *128*, 11006−11007.
(21) Sharma, J.; Chhabra, R.; Cheng, A.; Brownell, J.; Liu, Y.; Yan, H. *Science* **2009**, *323*, 112−116.
(22) Liu, N.; Liu, H.; Zhu, S.; Giessen, H. *Nat. Photonics* **2009**, *3*, 157−162.
(23) Kuzyk, A.; Schreiber, R.; Zhang, H.; Govorov, A. O.; Liedl, T.; Liu, N. *Nat. Mater.* **2014**, *13*, 862−866.
(24) Ma, W.; Kuang, H.; Wang, L.; Xu, L.; Chang, W.-S.; Zhang, H.; Sun, M.; Zhu, Y.; Zhao, Y.; Liu, L.; Xu, C.; Link, S.; Kotov, N. A. *Sci. Rep.* **2013**, *3*, 1934 DOI: 10.1038/srep01934.
(25) Zhang, S.; Zhou, J.; Park, Y.-S.; Rho, J.; Singh, R.; Nam, S.; Azad, A. K.; Chen, H.-T.; Yin, X.; Taylor, A. J.; Zhang, X. *Nat. Commun.* **2012**, *3*, 942.
(26) Decker, M.; Zhao, R.; Soukoulis, C. M.; Linden, S.; Wegener, M. *Opt. Lett.* **2010**, *35*, 1593.
(27) Rakic, A. D.; Djurišic, A. B.; Elazar, J. M.; Majewski, M. L. *Appl. Opt.* **1998**, *37*, 5271.
(28) Palik, E. D. *Handbook of Optical Constants of Solids*; Academic Press: San Diego, 2012.

DOI: 10.1021/acs.nanolett.5b03970
Nano Lett. 2015, 15, 8336−8341